NEW NITRIC OXIDE (NO) NIGHTGLOW MEASUREMENTS WITH SPICAM/MEX AS A TRACER OF MARS UPPER ATMOSPHERE CIRCULATION AND COMPARISON TO A MODEL.

J.L. Bertaux, F. Montmessin , *LATMOS/IPSL/CNRS, Université de Versailles Saint-Quentin, Guyancourt France (jean-loup.bertaux@latmos.ipsl.fr)* **F. Gonzalez-Galindo,** *Instituto de Astrofisica de Andalucia, CSIC Granada, 18080, Spain* **M.E. Gagné,** *Canadian Centre for Climate Modelling and Analysis, Environment Canada, University of Victoria, BC, Canada.*

Introduction:

The atmospheres of Venus and Mars have a similar composition (~95% CO_2 and 3-4% N_2), and therefore, we may expect some other similarities. In the thermospheres of both planets, CO_2 and N_2 molecules are photo-dissociated by solar UV and EUV radiation. O and N atoms are transported by the general circulation from the dayside to the nightside, where they recombine in O_2 and NO molecules, as recognized by their nightglow emission at 1.27 μm and in the UV respectively. These emissions are a direct tracer of the atmospheric dynamics and their study therefore provides a powerful diagnostic of the general circulation in the upper atmosphere. After the 2005 NO discovery (Bertaux et al., 2005), Cox et al. [2008] analyzed 21 orbits of SPICAM containing limb observations of these NO UV emissions: the maximum brightness of the observations is in the range 0.2 to 10.5 kiloRayleigh (kR), with a mean value of 1.2□1.5 kR, and it peaks between 55 and 92 km in altitude, with a mean value of 73.0 ± 8.2 km.

In the present work we have taken the approach of Royer et al. [2010] and scrutinized 2215 stellar occultations performed by SPICAM to look for "stray light" emission at the limb of Mars. We extracted NO signal from 128 of the 2215 occultations, allowing a much better global view than that from the rather sparse dedicated nightglow limb data (29 independent positive detections over two years 2004-2006 [Cox et al., 2008]). The present dataset extends from Ls= 44° for Martian year (MY) 27 to Ls=326° in MY 29, spanning almost 3 Martian years in total. In addition, we have developed an inversion technique (spatial/spectral deconvolution), which allows the retrieval of 2-D snapshot of the airglow layer brightness distribution within one occultation, projected at the limb (altitude and horizontal distance, because the spacecraft is also moving horizontally during one occultation). This abstract is a summary of a more extended paper [Gagné et al., 2013].

Observations :

Stellar occultation sequences from orbits 485 to 7237, which correspond to nearly three Martian years of observations, or six Earth years, have been examined. Of the 2215 occultations processed, 128 (□6%) produced a detectable NO emission (>0.5 kR). In the remaining sequences, the NO emission was lower than our detection limit in 1992 cases, and in 95 cases the result was uncertain because of light contamination, and therefore discarded from the present study. For each of the 128 occultations that returned a positive NO detection, we proceeded with the inversion technique described in the supplementary information provided. The resulting dataset extends the latitudinal and seasonal coverage beyond that of the data used in the Cox et al. [2008] study. On Figure 1 we have plotted all the positions of examined stellar occultations as a function of latitude and season (solar longitude Ls), folding in the three Martian years of data. Small black points indicate no positive detection, while positive detections are at colored symbols, with their peak horizontal (limb) intensities color coded. There is a clear seasonal pattern of colored circles, which is confirmed by the earlier SPICAM NO data from Cox et al. [2008] enclosed within a square. The brightest NO emission is found around a sine curve which may be described as latitude=-80 sin(Ls) [Bertaux et al., 2013], with however some serious departures from the sine curve in the second part of the Martian year (Ls=180-360°).

The model prediction of NO emission:

The results shown on figure 2 are the outputs of a one Martian year simulation with the Laboratoire de Météorologie Dynamique Mars General Circulation Model (LMD-MGCM). It simulates the horizontal intensity as would be viewed at the limb at its peak altitude, for a better comparison with SPICAM observations. The model is basically that described in Gonzalez-Galindo et al. [2009], but with an extended photochemical module including nitrogen and ionospheric chemistry from Gonzalez-Galindo et al. [2011] and an improved treatment of the non-local thermodynamic equilibrium 15-μm cooling that provides realistic temperatures in the mesopause region [Lopez-Valverde et al., 2011]. In total, 93 chemical reactions for the neutral upper atmosphere and the ionosphere are taken into account. This photochemical model is run for layers above 1 Pa (□50 km).

The structure of the latitude/season pattern may be explained with the following scenario as schematized on figures 4a and 4b. During solstices conditions, air is ascending on the summer pole, moves in a single Hadley cell to the winter night pole where it descend and CO_2 finally condenses at ground level.

During equinox conditions, air is ascending at equatorial latitudes and descends simultaneously on both poles in a two cells meridian circulation pattern. The pattern is quite similar to the O_2 model night emission (figure 3) produced by O+O→ O_2* → O_2 + 1.27 µm emission as detected first by OMEGA/Mars Express [Bertaux et al., 2012].

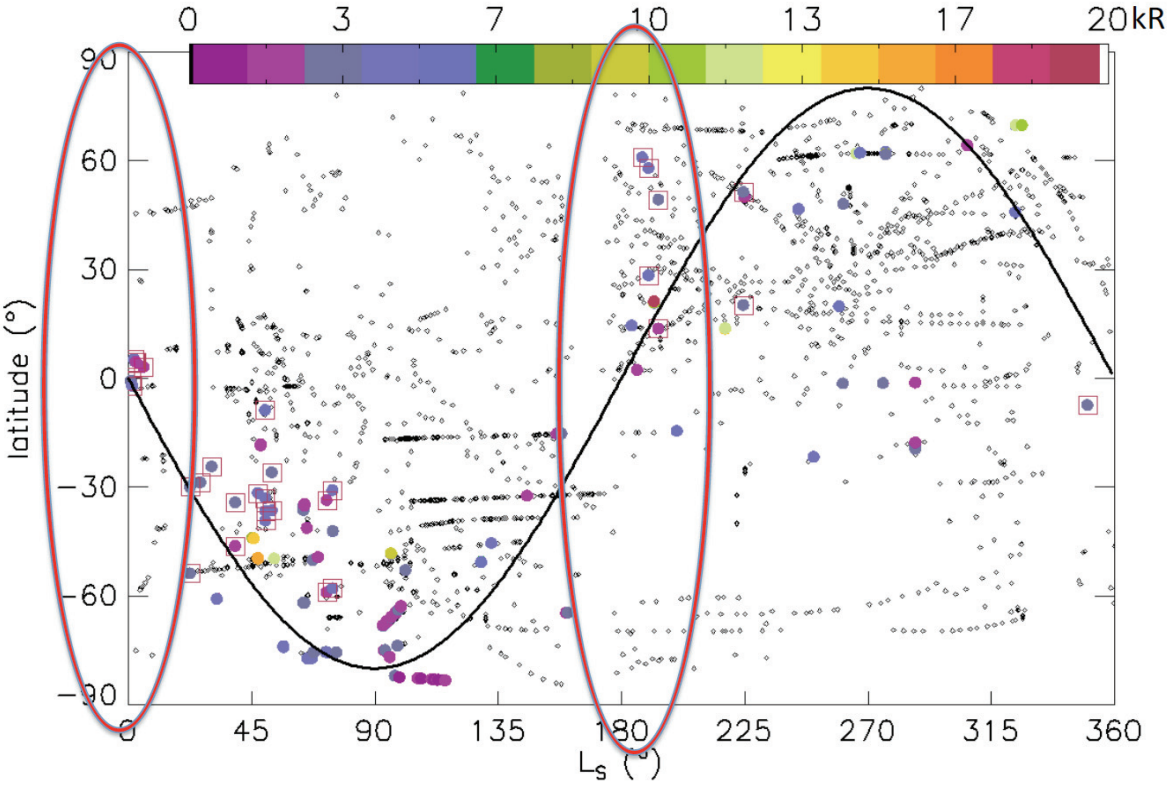

Figure 1. NO observations plotted as a function of Ls and latitude. Color dots overlaid with diamonds represent time and location of the positive detections during that interval, with the color coding the measured limb intensity in kR. Color dots overlaid with squares represent the time, location, and intensity of dedicated limb intensities extracted from Cox et al. [2008]. The black solid line is a sine curve, latitude=-80 x sin(Ls), along which fall (more or less) the positive NO detections of both datasets, this one and that of Cox et al. [2008]. Ellipses are for showing solstices.

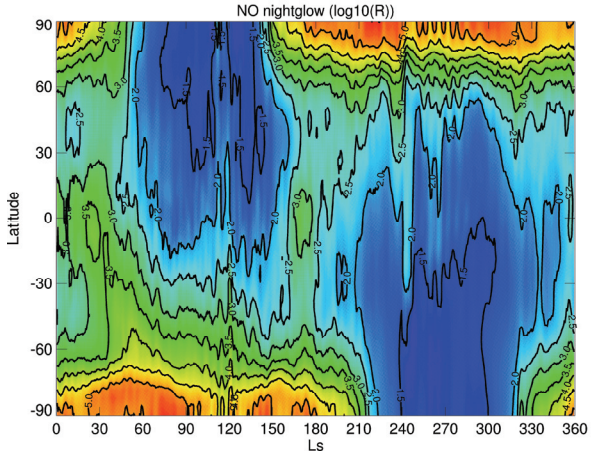

Figure 2. Zonal mean NO nightglow limb integrated intensity (Rayleigh) predicted by the LMD/MGCM as a function of latitude and Ls at LT=21. Note that the color scale is logarithmic: $3=10^3$ R.

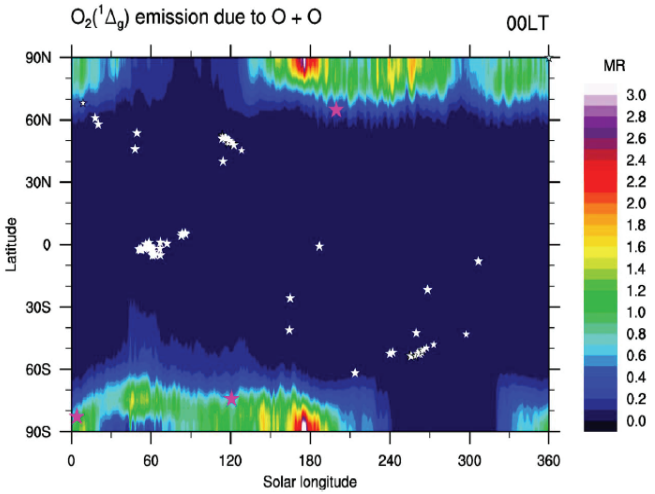

Figure 3. Zonally-averaged O_2 vertical emission produced by the O+O recombination (MegaRayleigh), as calculated by the LMD general circulation model. Locations where OMEGA detected an emission (3 pink stars) are in the regions where the model predicts a substantial intensity while observations without detection (white stars) are outside these regions.

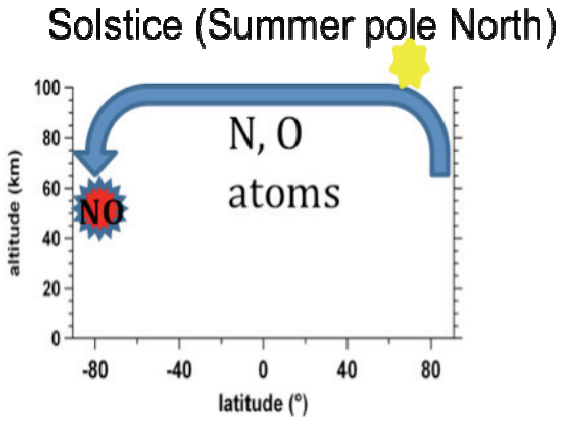

Figure 4a. During solstice conditions, the meridional circulation has one Hadley cell from summer to winter night. When descending, O and N atoms produce at high altitude are recombining to produce both the UV NO and NIR O_2 emissions.

Comparison for solstice conditions:

From the observations plotted in Figure 1, we see that during the Southern winter solstice (around Ls=90°) all positives detections between Ls=60° and Ls=120° are at latitudes southward of -30°. This is in agreement with the model prediction of Figure 2 that shows NO emissions above 1 kR for Ls=60-120° to be found at lat pole ward of -30°. The SPICAM detection limit in the present study is about 0.5 kR. However, for latitudes beyond -60°, the model predicts NO intensities above 10 kR and reaching more than 100 kR southward of 75°; the observations of NO intensities are then much weaker than the model results at high latitudes.

We note that SPICAM made stellar occultations around the Southern winter solstice at high latitudes for MY27 only. For the opposite solstice (Ls=240-300°), the agreement is less obvious: the detections are spread over a large latitude range, from -20 to +70°, while the model predicts a much weaker emission near the equator, and emissions of >1 kR to be located northward of +60°. Hence, in the Northern hemisphere, the observed NO emission region extends further towards the equator than the model predicts. Therefore, the NO data indicates an asymmetric situation between the Northern and Southern winter solstices, with the observed emissions more extended to lower latitudes for the Northern winter solstice, contrary to the prediction of the model. Another observed asymmetry (Figure 1) is that for Ls around 90°, almost all observations at latitude poleward of -70° contain some NO emission, while around Ls=270°, there are plenty of stellar occultations in the high Northern latitudes without a detectable signal from NO. The present analysis is somewhat biased by the more numerous positive detections recorded during year MY27, which might have been dynamically special. We note however that there are still four detections of NO emission at low latitudes (between -30 and +30°) during MY28 and MY29.

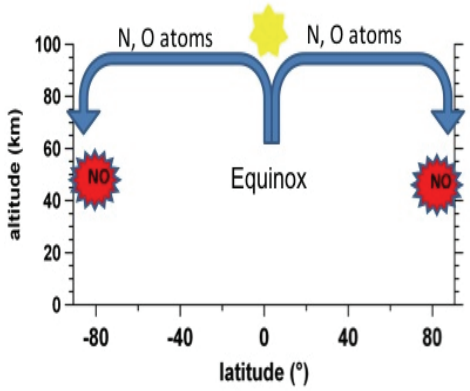

Figure 4b During equinox conditions, the meridional circulation has two Hadley cells. The model predicts emission simultaneously at both poles.

Comparison for equinox conditions.

The main discrepancy between the model and the observations is rather for equinox conditions, where the model predicts two maxima of emissivity located at both poles, while in the data, we did not detect high emissions at high latitudes, i.e., poleward of latitudes 60°, either around Ls=0° or Ls= 180°. For Ls=330-30°, there are no detection of NO emissions in either hemispheres, but SPICAM made only 8 stellar occultations sequences for lat>60° in both hemispheres, a region where the model predicts emissions detectable by this instrument. For the Ls=180° season, there were many stellar occultations at high latitudes (both in the Southern and Northern hemispheres), and only three of them showed a detection between Ls=150-210° (see Figure 1). For Ls=30-60°, the positive detections are at mid-latitudes. The model does predict an extended zone of dimmer but detectable (<1 kR but >0.5 kR) emission at mid- and low- latitudes for this season, as shown on Figure 2. However, at the other equinox (Ls=180°), the emission predicted by the model at mid-latitudes is less than 1 kR, while the observations show intensities of up to several kR. It has to be taken into account that the model results we are showing here are geographical (zonal mean) and temporal (during 30° of Ls) averages at a single local time (LT=21). The spatial and temporal variability can produce local enhancements of detectable emission, even if the average level predicted by the model is below 1 kR.

Conclusions: The NO intensities from LMD-MGCM are in general agreement with the observations, indicating that the main features of production of NO are captured by the model. We note however two important discrepancies between data and model that deserve further investigation. The first discrep-

ancy is the North-South asymmetry present in the data, which does not seem to be in the model. Three departures from symmetry may be visualized by the scatter of the observations from the sine curve -80x sin(Ls). Firstly, the "NO polar season" seems to be much shorter for the Southern hemisphere than for the Northern hemisphere. This is surprising since the Southern winter is longer than the Northern winter, due to orbit eccentricity. In the South, there are more than 50 detections poleward of -60°, while there are less than poleward of 60° in the North. Secondly, as noted above, the lowest altitude is increasing from the South pole to North pole.

We know that there is a major difference between the halves of the Martian year, the second half being the season of large dust storms. One might speculate that in the second part of the year, convection, which lifts dust to altitudes up to several tens of kilometres, is somewhat perturbing the descent of air from higher altitudes, triggering by compensation some descent of air at low latitudes where it is not predicted by the model. The second, and perhaps more important, discrepancy is the absence of simultaneous detections at both poles of a strong NO emission. Both model maps of NO and O_2 (Figure 3 from Bertaux et al. [2012]) indicate that, at the equinoxes, there is two simultaneous descent of air in both poles, revealing the existence of two Hadley cells in the thermosphere, extending from the equator to both poles. At other seasons, there is only one cell ascending from the summer hemisphere and descending in the polar regions where CO_2 is condensing on the ground. The strongest emissions in both the modeled NO and O_2 are at the equinoxes. While there are indeed observations of the O_2 emission at both poles during equinox conditions from CRISM data [Clancy et al., 2012], supporting the scheme of two cells for the O_2 emission, it seems that the same circulation pattern is not supported by the absence of detection of NO emission at the poles during equinox (at least at Ls=180°). This is rather surprising since the same circulation produces both O_2 and NO emissions. We note however two basic differences which might help to understand the discrepancy. N_2 requires more energetic photons (80-100 nm) than CO_2 for photodissociation and these photons are shielded by CO_2 absorption. Consequently, the altitude range of production of N atoms is above the bulk CO_2 atmosphere, at 130-140 km, as demonstrated by results from the photochemical model that includes nitrogen and ionospheric chemistry (not shown here). This is well above the altitude range of production of O atoms, with peaks at 70-90 km. Therefore, the discrepancies between the model and the observations suggest that it is the high altitude part of the GCM, relevant to the altitude range of N production, which would have to be adjusted. Another difference is that the O_2 recombination requires the presence of a CO_2 molecule to stabilize the reaction, but NO recombination does not. As discussed in Bertaux et al. [2012], an air parcel with a certain mixing ratio ρ, when descending, will produce an O_2 emission proportional to $\rho(O)^3$, while for NO, the emission will depend on the product of ρ(O) x ρ(N) and therefore will be less sensitive to descent of air. A more detailed investigation of these data-model discrepancies remains a potential topic for future work.

References:

Bertaux, J.-L., Leblanc, F., Perrier, S. Quemerais, E., Korablev, O., Dimarellis, E., Reberac, A., Forget, F., Simon, P. C., Stern, S. A., Sandel, B., Nightglow in the Upper Atmosphere of Mars and Implications for Atmospheric Transport, Science, 307,566 (2005).

Bertaux, J.-L., B. Gondet, F. Lefèvre, J.-P. Bibring, and F. Montmessin. First detection of O_2 1.27 μm nightglow emission at Mars with OMEGA/MEx and comparison with général circulation model predictions. Journal of Geophysical Research-Planets, 117:E00J04, 2012. doi: 10.1029/2011JE003890

Cox, C., A. Saglam, J.-C. Gérard, J.-L. Bertaux, F. Gonzalez-Galindo, F. Leblanc, and A. Reberac. Distribution of the ultraviolet nitric oxide Martian night airglow: Observations from Mars Express and comparisons with a one-dimensional model. Journal of Geophysical Research Planets, 113(E8):E08012, 2008. doi: 10.1029/2007JE003037.

Clancy, R. T., B. J. Sandor, M. Wolff, M. Smith, F. Lef evre , J.-B. Madeleine, F. Forget, S. Murchie, F. Seelos, K. Seelos, H. Nair, A. Toigo, D. Humm, D. Kass, A. Kleinböhl, and N. Heavens, Journal of Geophysical Research-Planets, 117:E00J10, 2012. doi: 10.1029/2011 JE004018.

Gagné, Marie-Eve, J.-L. Bertaux, F. González-Galindo, S. M. L. Melo, F. Montmessin, and K. Strong (2013), New nitric oxide (NO) nightglow measurements with SPICAM/MEx as a tracer of Mars upper atmosphere circulation and comparison with LMD-MGCM model prediction: Evidence for asymmetric hemispheres, J. Geophys. Res. Planets, 118, 2172–2179, doi:10.1002/jgre.20165.

Gonzalez-Galindo, F., Forget, M. A. Lopez-Valverde, M. Angelats F. i Coll, and E. Millour. Journal of Geophysical Research-Planets, 114:E04001, 2009. doi: 10.1029/2008JE003277.

Gonzalez-Galindo, F., A. Mäattanen, F. Forget, and A. Spiga. The Martian mesosphere as revealed by CO_2 cloud observations and General Circulation Modeling. Icarus, 216(1):10–22, 2011. ISSN 0019-1035. doi: 10.1016/j.icarus.2011.08.006

Lopez-Valverde, M. A., G. Sonnabend, M. Sornig, and P. Kroetz. Modelling the atmospheric CO_2 10-μm nonthermal emission in Mars and Venus at high spectral resolution. Planetary and Space Science, 59(10, SI):999–1009, 2011. ISSN 0032-0633. doi: 10.1016/j.pss.2010.11.011.

Royer, E., F. Montmessin, and J.-L. Bertaux. NO emissions as observed by SPICAV during stellar occultations. Planetary and Space Science, 58(10):1314–1326, 2010.